

Investigating the Edge Forming Performance of DP600 and FV 607

M. R. Allazadeh
A. Baker
J. S. Kwame

University of Strathclyde, Glasgow, United Kingdom

Abstract. This paper scrutinises the effect of varying test parameters on two grades of advanced high strength steels (AHSSs) prepared with abrasive water jet (AWJ) machining during hole expansion test (HET). The main objective was to understand the effect of the forming speed and the bottom die geometry on the hole edge forming performance of DP600 and FV 607 AHSSs. The results showed an optimum forming speed exists between 1 and 1.6mm/s and the FV 607 displayed better hole-expansion performance at 2mm/s. This was explained by correlation between the hole expansion ratio (HER) and the flange height. The results showed that the geometry of the bottom die have an influence on the hole-edge forming capability. The sheet thinning tendency was observed more in the bulge die, and particularly at speeds above 1 mm/s which was argued by requirement for larger HER values for more excessive thinning to account for an enhanced deformation. The FV 607 grade exhibited more thinning under all test conditions.

Key words: advanced high strength steels, abrasive water jet machining, forming parameters, hole expansion test.

Introduction

Steel has always been a key player in the automotive industry due to its versatility and low cost (Hilditch et al., 2015: 13-20). However, steelmakers have been progressively under pressure to optimise three main material attributes in the steel sheets to maintain their position in the automotive sector. These factors includes; developing material with better formability, higher strength and lower weight. A car body is mainly a large assembly of stamped sheet components from metal with good formability and crash performance. Lower strength steels (e.g. interstitial free (IF) and mild steels) have good total elongation attributes and are typically used in more complex shape components. Commonly, the formability of materials are judged with their yield and tensile strengths, r - value (the anisotropic plastic strain ratio) and n - value (the work hardening exponent) (Suzuki et al., 2018: 556-570). However, the requirements for safety and crashworthiness standards have informed the construction of automobile structural body parts from high-strength steel (HSS) sheets because of their higher strength compared to mild steels. Automotive components are often made from processes such as stamping and flanging. The use of such processes alongside HSS's poor formability is limiting the usage of steels which are employed almost exclusively in the automotive industry. This is as opposed to being used in body panels which are typically made from more formable steels (e.g. IF steels) which allow for the complex shapes and features to be implemented into vehicle design more easily (Atzema, 2016: 43). Thereof, the steel industry is investing substantial time, interest and money into the development of lightweight high strength steel to fend off competition from other lightweight materials such as aluminium alloys and composites. Their development was driven by pressure placed on the automotive industry to reduce vehicle emissions while at the same time improving vehicle safety. For this purpose, Advanced High Strength Steel (AHSS) were developed for use in the automotive industry. AHSSs

sometimes referred to as Ultra HSS, are as the name suggests a class of steel, which have ultimate strength values that are typically much larger than the average mild or low alloyed steels.

AHSSs exhibit superior performance due to their complex microstructure. More specifically, they exhibit significantly higher strengths than mild steels while offering global formability to match conventional HSS. While AHSSs display global elongation values similar to those displayed by conventional HSS, they suffer from poor local formability (e.g. edge cracking and tearing) (Huang and Singh, 2014). Some of the components that AHSSs are used in include A pillars, B pillars, Front and rear crash rails, Sill reinforcement and Roof rails (Billur and Altan, 2014: 16-17). Using AHSS in the mentioned components utilises their necessary properties such as high strength and excellent energy absorption capabilities (Hilditch et al., 2015: 13-20). Considerable AHSS productions are used in the automotive industry to comply with improved safety and reduced emissions. As result of this, and their lack of formability, they are typically used in structural and crash safety components.

Tests that are commonly used to characterise material behaviour (e.g. the uniaxial tensile test and form limiting curves (FLCs)) are not adequate for assessing the edge forming capability of AHSSs. This is because FLCs represent the limit of stretching but not bending or combined loading (Stamping Journal, 2008). The uniaxial tensile test cannot be used due to fundamental differences in deformation and damage mechanisms between the two tests (Paul, 2018: 2115). Many AHSSs exhibit adequate global formability but poor edge cracking performance (Huang and Singh, 2014). The Hole-Expansion Test (HET) was therefore developed to determine material edge formability. The standard mechanical test used for determining the edge forming performance of sheet metals are governed by BS ISO 16630:2017 (BSI, 2017). For a material with an initial hole diameter D_0 and a final hole diameter D_f after HET, the hole expansion ratio (HER) defines the extent of edge formability of the material. The HER is given by equation (1):

$$HER = \frac{D_f - D_0}{D_0} \times 100\% \quad (1)$$

The HER value can be used to rank materials based on their flangeability in order to assess their suitability for adoption in a particular automotive component fabrication. The HET was developed to determine the stretchability of sheet edges (BSI, 2017; Krempaszky et al., 2014: 204-209; Kim et al., 2018: 187-194) and characterise their resistance to edge cracking (Huang and Zhang, n/d). Several researchers have analysed the different parameters that affect the edge forming capability of AHSSs. Pathak et al. (2016: 4919) analysed the effect of punch geometry and burr orientation on HER. The results showed that using a conical punch produced larger HER values than using a flat punch. Similar impact of punch geometry on HER has been reported in other studies (Stachowicz, 2008: 167-172). The differences in punch geometry response was attributable to the variations in stress field produced at the hole edge. Chiriac and Chen (2008: 1-11) also varied the forming speed from 0.2-0.8mm/s and found that the HER increased with forming speed. Fang et al. (2003: 3877) demonstrated in their study that specimens with a greater thickness exhibited higher HER values. Other studies noted that at a critical clearance value of 20%, AHSS exhibited the best edge forming tendencies with the HER values decreasing with increasing material hardness (Mori et al., 2010: 653-659).

The aim of this study is to analyse the edge forming capability of two AHSSs for edges prepared with abrasive water jet machining using HET. The tool geometries adopted for this research are different from the standard tool dimensioning stipulated in BS ISO 16630:2017. However, the dimensioning for the centre hole disc samples were consistent with the standards. The effect of punch speed and bottom die geometry on AHSS edge formability were analysed and discussed in this research.

Experimental procedure

The materials

The materials studied in this research were DP600 dual phase steels and FV607 Ferritic steels, supplied by international steel manufacturer SSAB. DP600 are extensively used in a number of critical automotive components such as; floor panel, bonnet outer, cowl and floor reinforcements (Phongsai et al., 2016: 485-493). The sheet thicknesses of the supplied DP600 dual phase steels and FV607 Ferritic steels were 1.5mm and 2mm respectively. The accompanying chemical constituents of the alloys examined in this research are shown in Tables 1 and 2.

Table 1. Chemical composition: DP600 (wt.%)

C	Si	Mn	P	S	Cr	Mo	Ni	N	V
0.14	0.44	0.66	0.03	0.025	10.82	0.84	0.66	0.021	0.23

Table 2. Chemical composition: FV607 (wt.%)

C	Si	Mn	P	S	Al	Nb+Ti	Cr+Mo	B	Cu
0.12	0.4	1.6	0.025	0.01	0.015-1.5	0.1	1	0.005	0.2

Material preparation

A 100mm outer diameter spherical disc with a 10mm diameter centre hole was utilised to study the edge forming performance of the materials. The dimensioning used to fabricate the test samples were consistent with ISO 16630:2017. An Omax Maxiem 1515 abrasive water jet (AWJ) cutting machine was used to prepare the test samples for the HET examination. The machining parameters used to fabricate the test samples are shown in Table 3. The same machining parameters were used to prepare the test samples for both materials.

Table 3. Abrasive water jet cutting parameters

Tool offset (mm)	0.38
High pressure (bar)	3102.64
Low pressure (bar)	1378.95
Abrasive flow rate (Kg/min)	0.45
Average cutting speed (mm/s)	6.1

Hole expansion test

A Zwick/Roell BUP 1000 testing machine was used to examine the edge forming performance of the materials. A 20mm diameter spherical punch was used to deform the samples in this research. A blank holder force of 200kN was used to prevent the material from drawing-in during the deformation process. Grease was used as a lubricant to reduce friction at the punch-sheet metal interface during the testing process. The impact of tool geometry on HER was assessed by examining the influence of two different bottom die geometries. Fig. 1 shows the flat die and the bulge die. Prior to the deformation trials,

the initial hole diameters of the test samples were measured using a Mitutoyo IP67 coolant proof calliper. During the testing process, the punch exerts force at the pre-fabricated hole area until a through thickness crack occurred at the hole edge. A crack sensitivity sensor on the testing machine was activated to ensure rapid termination of the test upon the occurrence of the hole-edge cracks. The experiment was repeated for increasing punch speeds of 0.5, 0.8, 1.0, 1.6 and 2.0mm/s in order to ascertain their impact on the edge forming performance of the materials. The final hole diameter was measured after the test termination process. Based on the measured initial and final hole diameters, the HER of the examined materials were computed according to equation (1).

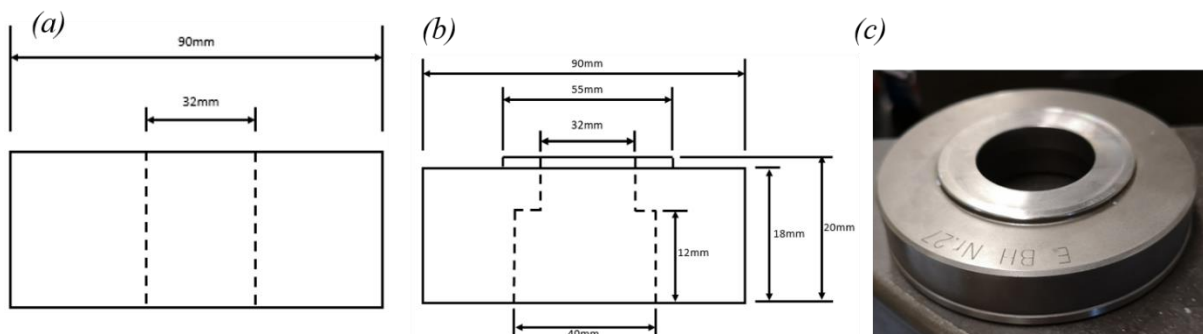


Fig. 1. Bottom die geometries: Schematics of the (a) flat and (b) bulge bottom dies, (c) image of bulge die

Results and Discussion

Hardness

The hardness values of both materials were measured and listed in Table 4. The FV 607 steel is significantly harder than the DP600. This trend may be attributed to the high martensite content of the FV 607 sheet material. The process and heat treatment history of the samples could also have an influence on the material hardness.

Table 4. Hardness measurements

Material	Hardness (HV)
DP600	176
FV 607	245

HER and flange height

Fig. 2 displays a plot of the average HER with different punch speeds for DP600 when deformed with two different bottom die geometries. From lower speeds up to 1.6mm/s, the flat die appears to produce better HER values compared to the bulge die. Excluding the results for the flat die at 0.8mm/s, HER appears to increase from lower speeds up to 1.6mm/s before decreasing significantly.

The difference in maximum and minimum HER is just over 30%. There is clearly an optimum forming speed somewhere between 1 and 1.6mm/s. Generally, it is assumed that with increasing strain rate the flow stress would increase and the sample would fail subsequently. This is clearly not the case in the curves of Fig. 2, and further investigation of material microstructure and properties may be required to explain this behaviour.

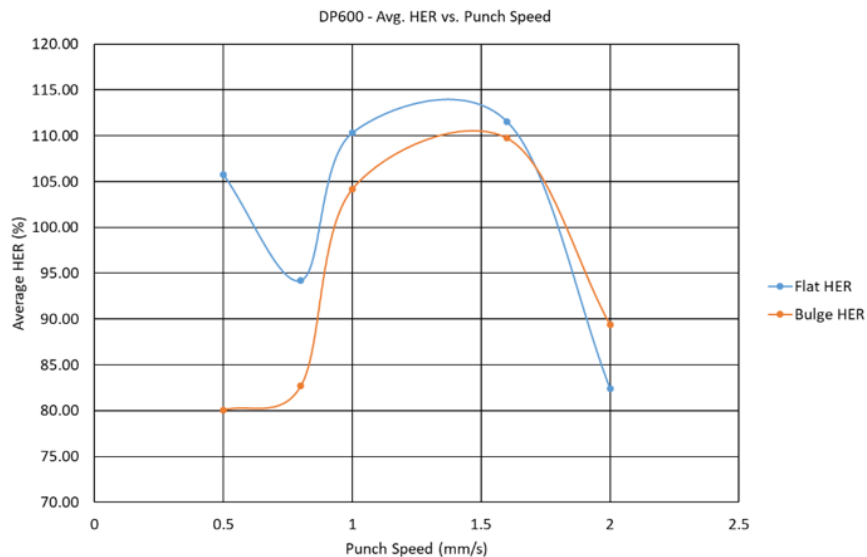


Fig. 2. Plot of average HER with punch speed (DP600)

Fig. 3 compares the performance of DP600 and FV 607 in terms of the HER, punch speeds and die geometries. About 1mm/s punch speed, there was essentially no significant difference in HER between the materials when deformed with flat die. However, for the bulge die DP600 exhibited higher edge forming capability compared to FV 607. At higher punch speed, e.g.2mm/s, FV 607 appeared to exhibit higher edge forming capability compared to DP 600 when examined with a bulge die by around 25%. The HER of FV 607 increased with speed when deformed with a bulge die.

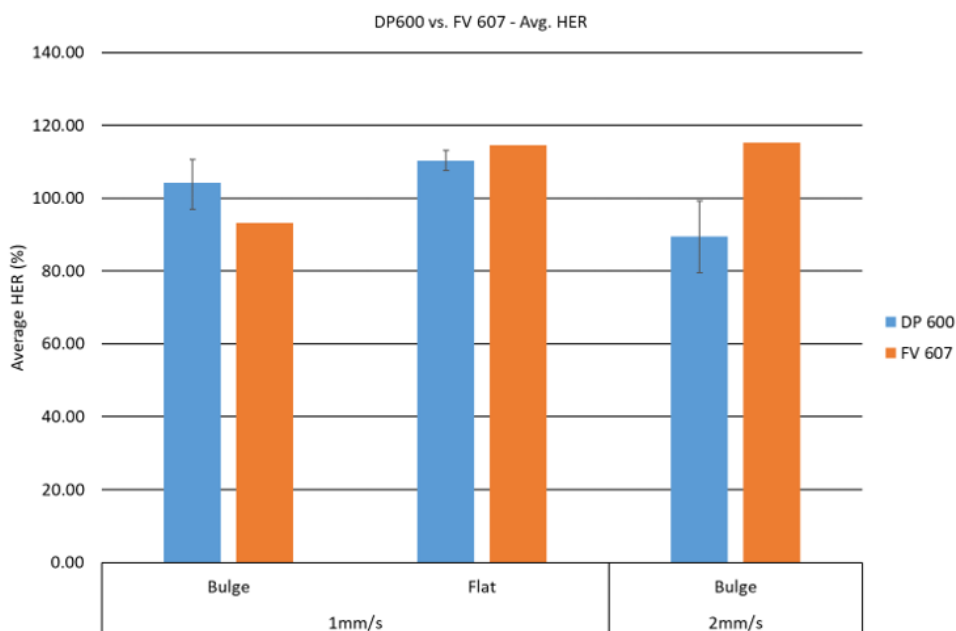


Fig. 3. Plot of HER with forming parameters

For the DP 600, the HER decreased at higher speeds when deformed with a bulge die. Based on literature review it was assumed that the DP steels would perform worse than the MS steel due to its complex and inhomogeneous microstructure. The FV 607 followed the expected trend of the HER increasing with forming speed and the strain rate.

HER values and the flange height evolution for DP600 after HET are shown in Fig. 4. There is clearly a positive correlation between the HER values and flange height. High HER values are representative of the high edge forming performance of the material, which were also visualised as higher flanges after the HET. The flange height evolution could therefore be considered as an indicator of edge forming performance of sheet metals.

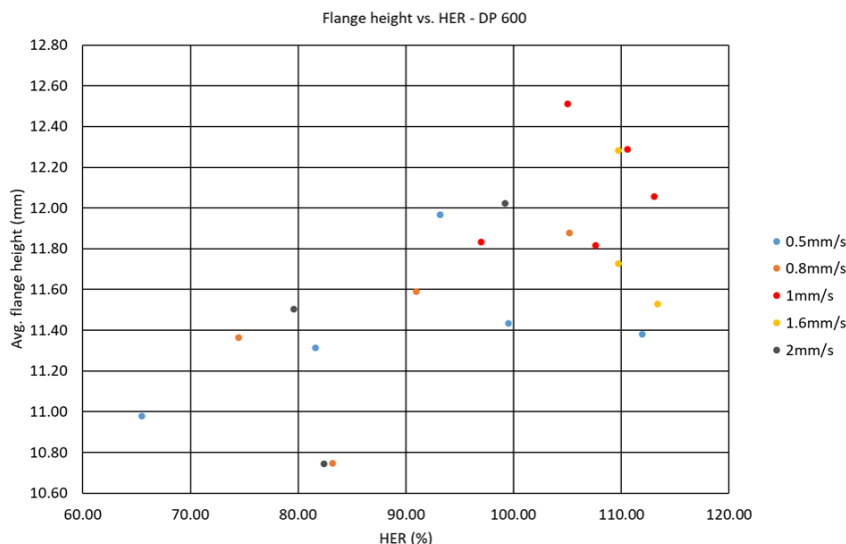


Fig. 4. Flange height and HER evolution in DP600

The flange height evolution with punch speed after HET of DP600 steel is shown in Fig. 5. The flange height increased with speed up to 1mm/s after which a reduction was observed with increasing punch speed for test conducted on both die geometries. At lower speeds (0.5-0.8mm/s), no significant difference in flange height was observed for the two die geometries. At higher speeds (1-2mm/s), the bulge die produced a higher flange when compared with the flat die. The ability of the bulge die to produce a higher flange may be attributable to the fact that only a small region of the specimen was clamped compared to the flat die. This meant that less material was restrained during deformation hence the trend.

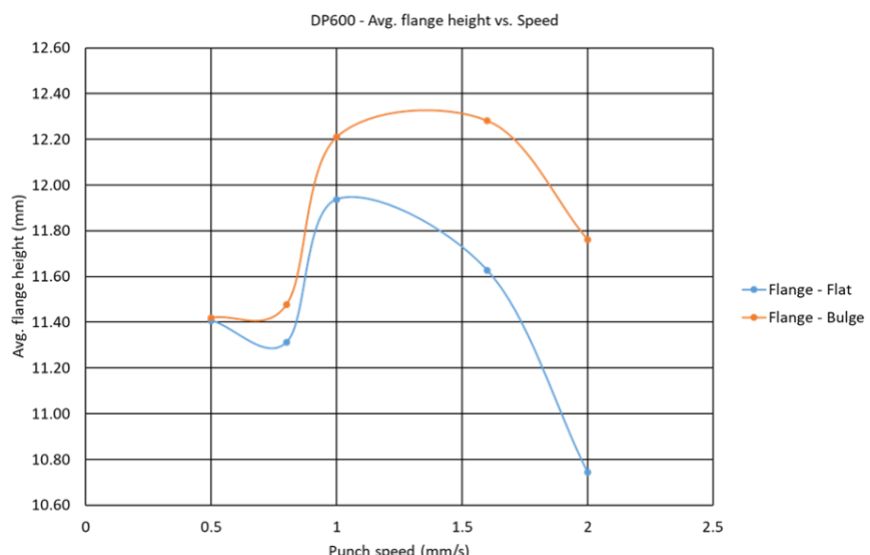


Fig. 5. Flange height evolution with punch speed for DP600 steels

Material thinning

Fig. 6 shows the results for the material sheet thinning evolution after HET plotted against the punch speed. Material thinning reaches a peak between 1 and 1.6mm/s, this is a consequence of the fact that larger HERs are produced at these speeds and since there is more expansion the specimen thickness reduces more to compensate. At lower speeds (0.5-0.8mm/s) the bulge flat die appeared to produce more thinning than the bulge die with the trend reversing for speeds greater or equal to 1mm/s.

The sheet thinning evolution observed in both materials at different testing conditions are shown in Fig. 7. The FV 607 steels exhibited higher thinning tendencies compared to DP600 steels. This difference was more pronounced for the samples tested at 1mm/s using the flat punch and at 2mm/s using the bulge punch. The difference in thinning response may be due to the variations in their inherent material metallurgical structure and edge surface microstructure response to AWJ machining.

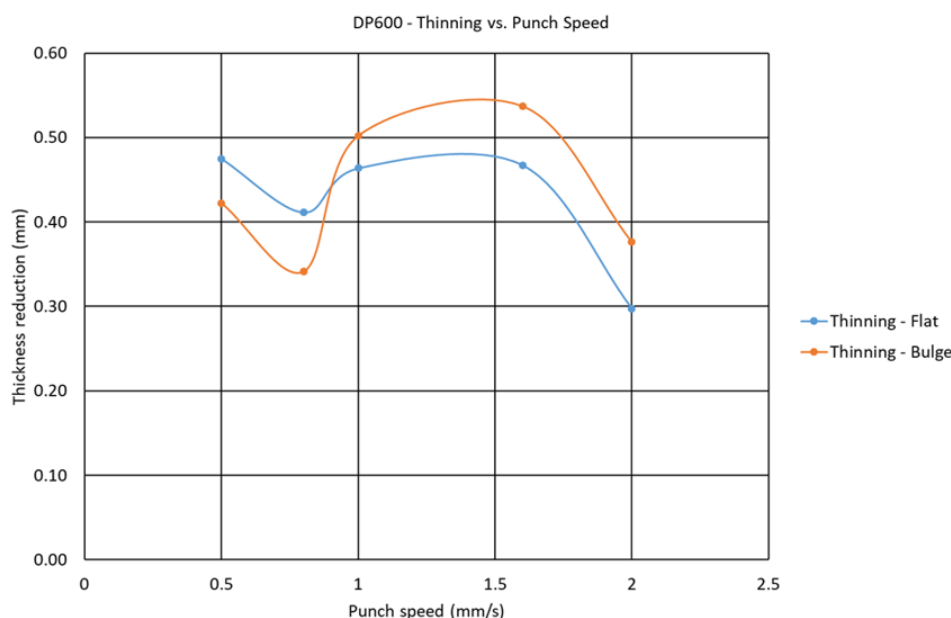


Fig. 6. Specimen thinning Vs. punch speed (DP600)

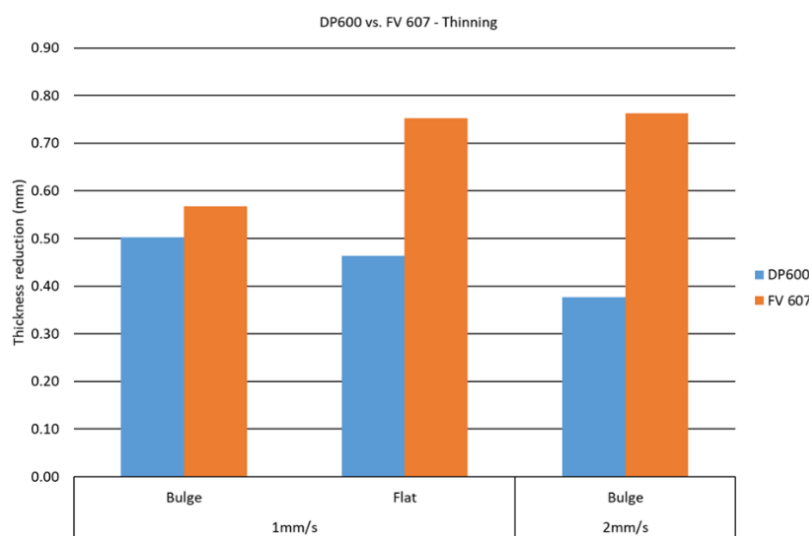


Fig. 7. Specimen thinning (DP600 VS. FV 607)

Errors during HET

Tool misalignment has been shown, in previous studies (Chiriac and Chen, 2008: 1-11), to have an effect on measured HER value. The maximum radial deviation has been plotted against variation in flange height for the corresponding individual specimens in Fig. 8. The variation in flange height was accounted for by taking the difference between the highest and lowest point of the flange on a specimen. Normally, variation in flange height increases with increasing tool misalignment and must be minimised where possible. Having a zero radial deviation is the ideal condition. However, this seldom occurs due to factors such as operator error and intrinsic machine misalignment caused by machining tolerances during manufacture. Die alignment tools could be used to minimise the risk during the experimental set-up step. The visual inspection of the tested samples in Fig. 9 reveals a skewed flanged in the direction of the misalignment which could influence the calculations of the flange height.

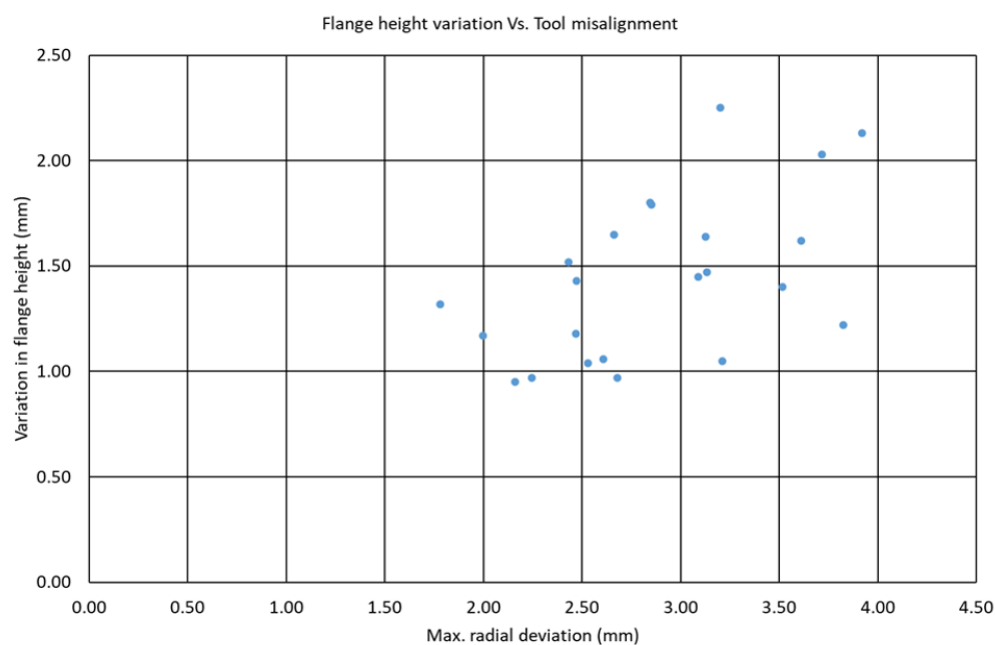


Fig. 8. Variation in flange height due to tool misalignment

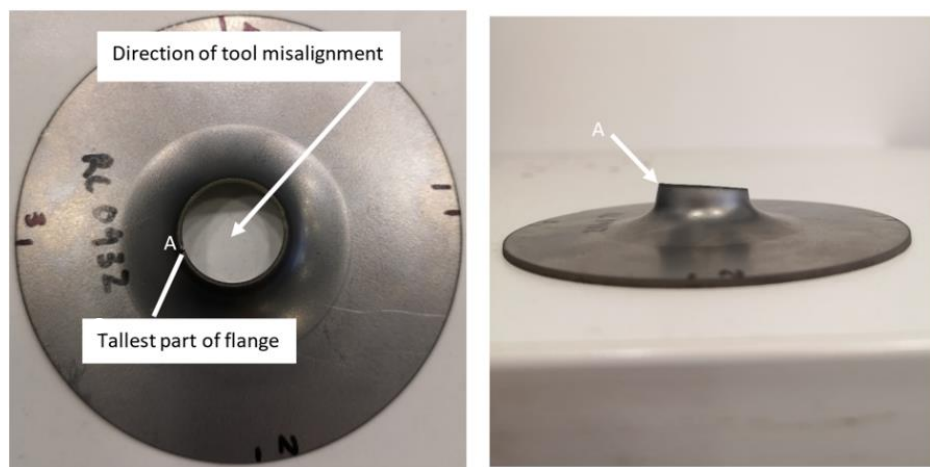


Fig. 9. Tool misalignment

Material spring back could also influence the HER values obtained in this research. Various researches have been directed at minimising the effect of spring back during metal forming processes (WorldAutoSteel, n/d). Material spring back is caused by internal stresses generated during material deformation. Reliance on operator instincts to terminate the test on the inception of edge cracks may also result in large variations in repeated test results.

Conclusion

This paper set out to analyse the effect of varying test parameters on two AHSSs using HET. By varying the punching speed it was discovered that an optimum speed exists between 1 and 1.6mm/s and the use of the flat die was also beneficial at these speeds. In terms of average HER, the FV 607 outperformed the DP600 at 2mm/s. At 1mm/s there was no significant difference in measured HER values. An optimum flange height also exists between 1 and 1.6mm/s. This is understandable since a positive correlation was observed between HER and flange height. For all speeds tested, the bulge die produced the highest flanges and it was suggested that this is due to it allowing more material flow. In terms of thinning, the bulge die produced more thinning at speeds above 1mm/s and more thinning was exhibited by the specimens which were tested using the bulge die. Again this is understandable, larger HER values require more excessive thinning to account for the deformation. Under all conditions the FV 607 exhibited more thinning compared to DP600. This could be due to the differences in their inherent material metallurgical structure or even the variations in their edge surface microstructure response to AWJ machining.

Further studies and larger number of HER tests should be conducted for better understanding of the HER attributes of the investigated materials and to aid in explaining the results obtained from the experimental analysis.

Acknowledgement

This research has been financially supported by the High Value Manufacturing (HVM) summer student internship at the Advanced Forming Research Centre (AFRC) of the University of Strathclyde. The authors are grateful for SSAB Swedish steel supports and AHSS sheets donation. The authors would like to thank Dr Yakushia and Dr Moturu for facilitating the experimental works of this project.

References

- Atzema, E.H. (2016). Formability of auto components. London: Elsevier Ltd.
- Billur, E., Altan, T. (2014). Three generations of advanced high strength steels for automotive applications, Part I. Stamp. J., December 2013-2014, 16-17. Available at: https://ercnsm.osu.edu/sites/ercnsm.osu.edu/files/uploads/S_FormingAHSS/664-1.pdf
- BSI. (2017). BS ISO 16630 : 2017 BSI Standards Publication Metallic materials – Sheet and strip – Hole expanding test.
- Chiriac, C., Chen, G. (2008). Local Formability Characterization of AHSS - Digital Camera Based Hole-expansion Test Development. International Deep Drawing Research Group IDDRG 2008 International Conference 16-18 June 2008, Olofström, Sweden, pp. 1-11.
- Fang, X., Fan, Z., Ralph, B., Evans, P., Underhill, R. (2003). The relationships between tensile properties and hole-expansion property of C-Mn steels. J. Mater. Sci., 38(18), 3877-3882. <https://doi.org/10.1023/A:1025913123832>

- Hilditch, T.B., de Souza, T., Hodgson, P.D. (2015). Properties and automotive applications of advanced high-strength steels (AHSS). London: Elsevier Ltd.
- Huang, M., Singh, J. (2014). A/SP Standardization of hole-expansion Test. Gt. Des. Steel. Available at: <https://docplayer.net/22014797-A-sp-standardization-of-hole-expansion-test.html>
- Huang, M., Zhang, L. (n/d). Standardization and Automation of Hole Expanding Test. Available at: https://www.academia.edu/8976871/Standardization_and_Automation_of_Hole_Expanding_Test
- Kim, J.H., Kwon, Y.J., Lee, T., Lee, K.A., Kim, H.S., Lee, C.S. (2018). Prediction of hole-expansion ratio for various steel sheets based on uniaxial tensile properties. Metals and Materials International, 24(1), 187-194. <https://doi.org/10.1007/s12540-017-7288-2>
- Krempaszky, C., Larour, P., Freudenthaler, J., Werner, E. (2014). Towards More Efficient Hole-expansion Testing. IDDRG 2014 Conference June 1-4, 2014, Paris, France, pp. 204-209. Available at: http://www.iddrg.com/mm/14/C_30_14.pdf
- Mori, K., Abe, Y., Suzui, Y. (2010). Improvement of stretch flangeability of ultra high strength steel sheet by smoothing of sheared edge. J. Mater. Process. Technol., 210(4), 653-659. <https://doi.org/10.1016/j.jmatprotec.2009.11.014>
- Pathak, N., Butcher, C., Worswick, M. (2016). Assessment of the Critical Parameters Influencing the Edge Stretchability of Advanced High-Strength Steel Sheet. J. Mater. Eng. Perform., 25(11), 4919-4932. <https://doi.org/10.1007/s11665-016-2316-9>
- Paul, S.K. (2018). Fundamental aspect of stretch-flangeability of sheet metals. Proc. Inst. Mech. Eng. Part B J. Eng. Manuf., 233(10), 2115-2119. <https://doi.org/10.1177%2F0954405418815370>
- Phongsai, T., Julsri, W., Chongthairungruang, B., Suranuntchai, S., Jirathearanat, S., Uthaisangsuk, V. (2016). Identification of material parameters for springback prediction using cyclic tension-compression test. Songklanakarin J. Sci. Technol., 38(5), 485-493.
- Stachowicz, F. (2008). Estimation of hole-flange ability for deep drawing steel sheets. Arch. Civ. Mech. Eng., 8(2), 167-172. [https://doi.org/10.1016/S1644-9665\(12\)60203-9](https://doi.org/10.1016/S1644-9665(12)60203-9)
- Stamping Journal. (2008). R&D Update: Examining edge cracking in hole flanging of AHSS. Available: <https://www.thefabricator.com/article/stamping/r-d-update-examining-edge-cracking-in-hole-flanging-of-ahss>
- Suzuki, T., Okamura, K., Capilla, G., Hamasaki, H., Yoshida, F. (2018). Effect of anisotropy evolution on circular and oval hole expansion behavior of high-strength steel sheets. International Journal of Mechanical Sciences, 146-147, 556-570. <https://doi.org/10.1016/j.ijmecsci.2017.10.038>
- WorldAutoSteel. (n/d). Dual Phase (DP) Steels. Available at: <https://www.worldautosteel.org/steel-basics/steel-types/dual-phase-dp-steels/>